Published in final edited form as:
Mol Microbiol. 2011 November ; 82(3): 664–678. doi:10.1111/j.1365-2958.2011.07842.x.

Late endosomal Rab7 regulates lysosomal trafficking of endocytic but not biosynthetic cargo in *Trypanosoma brucei*

Jason S. Silverman[1], **Kevin J. Schwartz**[1], **Stephen L. Hajduk**[2], and **James D. Bangs**[1,*]

[1]Department of Medical Microbiology and Immunology, University of Wisconsin School of Medicine and Public Health, Madison, WI 53706, USA

[2]Department of Biochemistry and Molecular Biology, University of Georgia, Athens, GA 30602, USA

Summary

We present the first functional analysis of the small GTPase, TbRab7, in *Trypanosoma brucei*. TbRab7 defines discrete late endosomes closely juxtaposed to the terminal p67^{+} lysosome. RNAi indicates that TbRab7 is essential in bloodstream trypanosomes. Initial rates of endocytosis were unaffected, but lysosomal delivery of cargo, including tomato lectin (TL) and trypanolytic factor (TLF) were blocked. These accumulate in a dispersed internal compartment of elevated pH, likely derived from the late endosome. Surface binding of TL but not TLF was reduced, suggesting that cellular distribution of flagellar pocket receptors is differentially regulated by TbRab7. TLF activity was reduced approximately threefold confirming that lysosomal delivery is critical for trypanotoxicity. Unexpectedly, delivery of endogenous proteins, p67 and TbCatL, were unaffected indicating that TbRab7 does not regulate biosynthetic lysosomal trafficking. Thus, unlike mammalian cells and yeast, lysosomal trafficking of endocytosed and endogenous proteins occur via different routes and/or are regulated differentially. TbRab7 silencing had no effect on a cryptic default pathway to the lysosome, suggesting that the default lysosomal reporters p67ΔTM, p67ΔCD and VSGΔGPI do not utilize the endocytic pathway as previously proposed. Surprisingly, conditional knockout indicates that TbRab7 may be non-essential in procyclic insect form trypanosomes.

Introduction

African trypanosomes (*Trypanosoma brucei* ssp.) are parasitic protozoa that cause human and veterinary trypanosomiasis throughout sub-Saharan Africa. The parasite life cycle alternates between the mammalian host and the tsetse fly vector, and two developmental stages are amenable to molecular and cell biological studies, the pathogenic mammalian bloodstream form (BSF) and the procyclic insect form (PCF). BSF trypanosomes live

*For correspondence. jdbangs@wisc.edu; Tel. (+1) 608 262 3110; Fax (+1) 608 262 8418.

Supporting information

Additional supporting information may be found in the online version of this article.

Please note: Wiley-Blackwell are not responsible for the content or functionality of any supporting materials supplied by the authors. Any queries (other than missing material) should be directed to the corresponding author for the article.

exclusively in the bloodstream and extracellular fluids where they avoid the host immune response by the well-documented process of antigenic variation (Schwede and Carrington, 2010). Also, important for BSF pathogenesis is the lysosome, which is critical for degradation of serum derived proteins for nutritional purposes (Langreth and Balber, 1975), and perhaps as a mechanism to eliminate potentially lytic cell surface immune complexes (Balber *et al*., 1979; Barry, 1979; Pal *et al*., 2003). Conversely, the activity of trypanolytic factor (TLF), a human serum innate immune complex that prevents infection with *T. b. brucei* (Hajduk *et al*., 1989; Vanhamme *et al*., 2003), is critically dependent on lysosomal function (Hager *et al*., 1994; Shimamura *et al*., 2001; Peck *et al*., 2008). Both endocytic and lysosomal activities are upregulated in BSF trypanosomes (Langreth and Balber, 1975; Pamer *et al*., 1989; Morgan *et al*., 2001), and lysosomal enzymes have been proposed as targets for chemotherapeutic intervention (Selzer *et al*., 1999).

Trypanosomes are highly polarized cells with a unique architecture (Engstler *et al*., 2006). All of the key organelles associated with eukaryotic secretory and endocytic trafficking are located between the central nucleus and the posterior flagellar pocket, the entry/exit point for all macromolecular cargo. Included in this repertoire of organelles are ER exit sites, the Golgi, a single terminal lysosome, and the core eukaryotic endosomal compartments, early, recycling and late. These organelles are present in reduced copy number compared with mammalian cells suggesting streamlining for efficient transport, and perhaps representing the basal trafficking requirements for such an early branching eukaryote.

There are at least two pathways to the lysosome in trypanosomes – the endocytic route from the flagellar pocket via endosomes, and the biosynthetic route from the Golgi. These pathways share features with higher eukaryotes including the use of clathrin, which mediates vesicular transport at the flagellar pocket (Allen *et al*., 2003), the recycling endosome (Grünfelder *et al*., 2003) and the Golgi (Tazeh *et al*., 2009). Studies with fluid phase markers, GPI-anchored variant surface glycoprotein (VSG), and receptor-mediated endocytic markers such as transferrin (Tf) (Grünfelder *et al*., 2003; Pal *et al*., 2003; Engstler *et al*., 2004) show that endocytic cargo sorts from the flagellar pocket to the early endosome and then on to the recycling endosome. From here, VSG and Tf receptor return to the plasma membrane via the flagellar pocket. Also present, but less well documented, is a recycling pathway leading from the early endosome to the late endosome, and then back to the recycling endosome (Engstler *et al*., 2004). Cargo destined for degradation, for instance Tf or host-derived antibodies, can be sorted to the lysosome at either the early or recycling endosomes. Lysosomal delivery presumably occurs via the late endosome, but this pathway is not well defined (Engstler *et al*., 2004).

Flux through the various endosomal compartments is controlled in part by specific Rab proteins, small GTPases that regulate vesicular transport in the eukaryotic endomembrane system (Seabra and Wasmeier, 2004; Grosshans *et al*., 2006), and trypanosomes have the common eukaryotic endosomal Rabs: TbRab5A/B, early endosome (Pal *et al*., 2002; 2003); TbRab11, recycling endosome (Hall *et al*., 2005); and TbRab7, late endosome (Engstler *et al*., 2004). Mutational and RNAi studies of TbRab5A/B and TbRab11 indicate that they regulate sorting through the early and recycling endosome as occurs in mammalian cells. However, other than localization studies indicating that the late endosome is a discrete

compartment in close proximity to the terminal lysosome (Engstler *et al*., 2004), no functional studies of TbRab7 and its role in lysosomal trafficking have been performed in trypanosomes.

The biosynthetic route to the lysosome has been defined in PCF trypanosomes using the lysosomal membrane protein, p67, and the soluble thiol protease, TbCatL. p67 is a type I membrane glycoprotein that is targeted from the Golgi to the lysosome by C-terminal di-leucine motifs (Alexander *et al*., 2002; Tazeh and Bangs, 2007). Similarly, post-Golgi transport of TbCatL requires recognition of specific signals in the prodomain by an as-of-yet uncharacterized sorting receptor (Huete-Perez *et al*., 1999; Tazeh *et al*., 2009). Lysosomal transport of both proteins is dependent on the AP-1/clathrin machinery in PCF trypanosomes, but the situation is less clear in BSF parasites (Tazeh *et al*., 2009). Deletion of the p67 cytoplasmic domain alone, containing the critical di-leucine motifs, or of the transmembrane and cytoplasmic domains together, had no effect on lysosomal targeting in BSF trypanosomes (Alexander *et al*., 2002). Furthermore, post-Golgi trafficking of both native p67 and TbCatL is unimpaired by silencing of the AP-1 machinery (Allen *et al*., 2007; Tazeh *et al*., 2009). A similar mistargeting phenomenon occurs in BSF trypanosomes with GPI-anchored VSG and TfR. These proteins are normally targeted to the plasma membrane, but elimination of the GPI anchor creates soluble proteins that are quantitatively misdirected to the lysosome (Böhme and Cross, 2002; Biebinger *et al*., 2003; Triggs and Bangs, 2003; Schwartz *et al*., 2005). The pattern that emerges is that in the absence of normal trafficking signals secretory proteins in BSF trypanosomes are targeted by default to the lysosome. As we have argued elsewhere (Tazeh *et al*., 2009), this does not mean that normal lysosomal targeting is inoperative in BSF trypanosomes. Rather it suggests that there is a cryptic lysosomal route that is exposed when normal trafficking is interdicted. Interestingly this default pathway is developmentally regulated as disruption of both signals and machinery results in quantitative secretion in PCF trypanosomes (McDowell *et al*., 1998; Alexander *et al*., 2002; Tazeh and Bangs, 2007; Tazeh *et al*., 2009).

The actual pathways for normal biosynthetic and default post-Golgi sorting to the lysosome are unclear. In PCF trypanosomes, where normal lysosomal trafficking is AP-1/clathrin dependent, the likely route is transport to the late endosome from which cargo is forwarded to the lysosome, but this has not been formally established. This would be similar to the situation in mammalian cells (Braulke and Bonifacino, 2009; Saftig and Klumperman, 2009), and as argued above, this is likely to be true also in BSF parasites. On the other hand, default trafficking in BSF trypanosomes is AP-1/clathrin-independent. We have proposed that default cargo leaves the Golgi via the secretory pathway, which is also AP-1/clathrin-independent, but that it intercepts the endocytic pathway and is swept back to the lysosome by bulk membrane flow (Tazeh *et al*., 2009). Again one would predict that this route traverses the late endosome. In this work we now use RNAi silencing of TbRab7 to investigate these unresolved issues. Our purpose is twofold – to perform a first detailed analysis of TbRab7 function in trypanosomes, and to probe the three routes to the lysosome: endocytic, biosynthetic and default. Our findings contrast strikingly with the function of Rab7 in mammalian cells and yeast, and also challenge our proposed route of default lysosomal trafficking in BSF trypanosomes.

Results

TbRab7 location

Although no functional studies have been published, previous work in BSF trypanosomes has localized TbRab7 to the late endosome in close proximity to the lysosome (Engstler *et al*., 2004). Consistent with this location we observed anti-TbRab7 staining juxtaposed to the lysosome as defined by the marker membrane protein p67 (Fig. 1A). In addition, a similar pattern of staining was observed in a cell line containing a Ty-epitope tagged chromosomal allele of TbRab7 (Fig. 1B). A tagged protein of expected size was specifically detected in these cells by Western blotting (Fig. S1). Finally, the same pattern of staining was seen with antibody to native TbRab7 in PCF trypanosomes (Fig. S2). These results confirm the TbRab7^{+} late endosome to be a discrete subcellular compartment in close association with the terminal lysosome in both the BSF and PCF stages of the *T. brucei* life cycle.

TbRab7 expression, and silencing

As expected for a core endocytic Rab, northern analysis indicates that TbRab7 is constitutively expressed in both BSF and PCF stages of the parasite life cycle (Fig. 2A). Multiple mRNA species were detected, including a closely spaced doublet of similar abundance, and a single less abundant high molecular weight species. There are no significant stage-specific differences in the expression levels of any of these species, consistent with all available transcriptome analyses (Aslett *et al*., 2010). Data presented below indicate that these RNA species all are derived from the native TbRab7 locus (Fig. 3). The doublet may represent alternate mRNA processing, and the high molecular weight species may represent dicistronic intermediates in mRNA processing (Tschudi and Ullu, 1988).

Silencing with an inducible stem-loop RNAi construct specifically reduced the steady state levels of TbRab7 message in BSF trypanosomes by 91.5 ± 8.0% (n = 3) after 28 h and likewise by > 90% PCF cells after 72 h (Fig. 2A). No gross morphological defects were observed via light microscopy in either stage at these times (data not shown). After induction of TbRab7 dsRNA BSF cell growth ceased at ~24 h, following which cells with abnormal morphology progressively accumulated with cell death ensuing by 48 h (Fig. 2B). Repeated attempts by western analysis to confirm ablation of TbRab7 protein in BSF trypanosomes were unsuccessful due to lack of a specific TbRab7 signal on blots; however, the specific signal in immunofluorescence was completely ablated (Fig. S3). These results suggest that TbRab7 function is essential in BSF trypanosomes. Surprisingly TbRab7 is apparently non-essential in PCF cells as no growth defect was observed in RNAi cells (Fig. 2B), even after 3 weeks of continuous induction (data not shown). This issue was further investigated by conditional double knockout of the TbRab7 locus in PCF trypanosomes. First one allele was replaced with a selectable drug marker to generate a single knockout (1KO) cell line. After addition of an ectopic inducible copy of TbRab7 to the cell line, the second native allele was replaced with a second selectable drug marker to generate a conditional double knockout (cKO) cell line. Replacement of the two alleles was validated by PCR amplification of the TbRab7 locus from genomic DNA from each cell line (Fig. 3A). In the 1KO cell line the native wild-type TbRab7 amplicon (773 nts) was reduced

approximately twofold relative to wild-type cells, and an additional amplicon of the expected size (2060 nts) for the replacement allele appeared. In the cKO cell line the native amplicon completely disappeared while a new amplicon (1860 nts) from the second replacement allele appeared, confirming knockout of both native alleles of TbRab7. Next tetracycline was withdrawn from the cKO cell line to terminate expression of the conditional copy of TbRab7. Northern analysis revealed the complete shutdown of inducible TbRab7 transcription at 6 days (Fig. 3B). In addition, none of the endogenous RNA species (Fig. 2A) were seen in the cKO cell line, confirming that all three are derived from the native TbRab7 locus. Despite the absence of all detectable TbRab7 mRNA cell growth was relatively unimpaired. An ~16% decrease in doubling time was seen from days 3 to 9 of conditional knockout, but normal growth returned after 9 days (Fig. 3C). This delayed growth phenotype and its recovery were reproducible in multiple experiments, and were also observed in a second clonal cKO cell line (data not shown). These data strongly suggest that TbRab7 is non-essential for sustained growth and viability of cultured PCF trypanosomes. However, a caveat to this conclusion is addressed in the *Discussion*. All subsequent phenotypic analyses were performed in BSF parasites at 28 h of silencing due to the efficiency of knockdown without overt morphological defects.

TbRab7 is essential for BSF endocytic lysosomal trafficking

To analyse the role of TbRab7 in endocytic trafficking, we used fluorescent imaging (Fig. 4) and flow cytometry (Fig. 5) with tomato lectin (TL) as a surrogate marker for receptor-mediated endocytosis. TL binds poly-N-acetyllactosamine (pNAL) epitopes on membrane glycoproteins in the flagellar pocket, e.g. Tf receptor, and is subsequently endocytosed and delivered to the lysosome (Nolan *et al*., 1999; Alexander *et al*., 2002). In both live control and TbRab7 silenced cells, TL bound in the flagellar pocket as indicated by localization immediately anterior to the kinetoplast (Fig. 4A and B). As expected, internalized TL colocalized with the lysosomal marker p67 in control cells (Fig. 4C). In contrast, in TbRab7 silenced cells endocytosed TL had a dispersed, punctate and distinctly non-lysosomal localization (Fig. 4D), but there was no apparent effect on lysosomal morphology. To confirm this at the ultrastructural level TbRab7 RNAi cells were preloaded with TL:colloidal gold to mark the terminal lysosome. TbRab7 silencing was then induced for 28 h and cells were examined by electron microscopy (Fig. S4). Normal lysosomes labelled in this manner typically present as 250–300 nm vacuoles with internal gold particles (Peck *et al*., 2008). This presentation was seen in both control and silenced cells confirming that lysosomal morphology was unaltered by TbRab7 ablation.

These qualitative results show that TbRab7 silencing does not prevent binding/uptake of endocytic cargo, but does alter its final destination after internalization, indicating that lysosomal delivery is impaired. However, quantitative analyses by flow cytometry revealed reduction of both TL binding (~ 41%) and uptake (~ 64%) in TbRab7 silenced cells compared with control cells (Fig. 5A). The actual rate of endocytosis was measured using TL:FITC as a pH-sensitive probe (Fig. 5B). FITC fluorescence is rapidly quenched as the fluor is internalized into acidified endosomes and delivered to lysosomes (Poole and Ohkuma, 1981), which in trypanosomes have an internal pH of 4.8 (McCann *et al*., 2008). As previously reported (Tazeh *et al*., 2009), as TL:FITC was internalized into control cells

fluorescent intensity decreased over time and then plateaued, representing transit of endosomes followed by arrival in the terminal acidified lysosome (Fig. 5B). The initial rate of uptake was unaffected by TbRab7 silencing (Fig. 5B, insert), but the final fluorescent intensity was elevated indicating delivery to a compartment of higher internal pH. Collectively, these results demonstrate that TbRab7 silencing does not affect internalization at the flagellar pocket, but does block delivery to the terminal lysosome. Instead endocytosed cargo is arrested in a dispersed pre-lysosomal compartment(s) of higher internal pH.

TbRab7 silencing reduces surface levels of transferrin receptor

The reduced binding of TL to live cells could be due to impaired addition of pNAL epitopes to N-glycans on resident flagellar pocket proteins and/or reduced levels of such proteins. First, to determine if TbRab7 silencing affects steady-state levels of total pNAL-modified proteins, whole cell extracts were blotted using TL as the probe (Fig. 6A). As seen by Nolan *et al*. (1999), TL recognized multiple proteins from middle to high molecular weight in control cells. An identical spectrum of pNAL-containing proteins was observed in TbRab7 silenced cells, indicating that ablation of TbRab7 does not affect pNAL glyco-modification in the Golgi. Another possible explanation for the decrease in TL binding is that silencing specifically alters the steady-state level of pNAL-containing proteins within the flagellar pocket, the best characterized of which is Tf receptor (TfR), a heterodimer of ESAG7 and ESAG6 (Ligtenberg *et al*., 1994; Steverding *et al*., 1994). Western blotting (Fig. 6B) and immunofluorescence (IFA) (not shown) of control and silenced cells revealed no obvious differences in expression or cellular distribution of TfR. We next used surface biotinylation to determine the relative amount of external TfR in control and TbRab7 silenced cells (Fig. 6C). In each case equivalent biotinylation of VSG, but not cytoplasmic HSP70 was seen, confirming both specific labelling of surface proteins and plasma membrane integrity. Biotinylation of TfR was also observed in each case, but was greatly reduced in TbRab7 ablated cells, indicating that silencing does lower the steady-state level of pNAL-containing membrane proteins in the flagellar pocket.

TbRab7 controls killing by TLF

We next investigated endocytosis of TLF, both as a natural ligand, and because of its role in the natural biology of human African trypanosomiasis. TLF is an innate immune factor that restricts human infectivity by *T. b. brucei*. A subspecies of human HDL (Rifkin, 1978; Hajduk *et al*., 1989), TLF is internalized by receptor-mediated endocytosis at the flagellar pocket (Drain *et al*., 2001; Shimamura *et al*., 2001; Vanhollebeke *et al*., 2008) and trafficked to the lysosome (Hager *et al*., 1994; Shimamura *et al*., 2001), resulting in eventual cell lysis. Normal lysosomal function is critical for TLF activity (Hager *et al*., 1994; Peck *et al*., 2008), and it is logical that impaired lysosomal delivery would also decrease trypanolysis. As seen with TL, fluorescent microscopy (Fig. 7A) revealed normal binding in the flagellar pocket in both control and silenced cells, but TbRab7 ablation prevented ultimate delivery of TLF to the lysosome. Instead, as with TL, internalized TLF was found in a dispersed non-lysosomal location. Failure to reach the lysosome corresponded to an approximately threefold decrease in the rate of killing following a typical initial lag phase (Fig. 7C). Unlike TL, however, flow cytometry revealed no quantitative changes in TLF binding or uptake (Fig. 7B),

indicating that TbRab7 silencing differentially affects the steady-state level of specific flagellar pocket receptors, e.g. transferrin vs. TLF. Overall, these results indicate TbRab7 broadly mediates lysosomal delivery of endocytosed proteins, and furthermore directly confirm that lysosomal delivery is critical for TLF activity.

TbRab7 is not required for biosynthetic lysosomal trafficking

The role of TbRab7 in biosynthetic trafficking to the lysosome was investigated using TbCatL, a soluble lysosomal thiol protease (Caffrey and Steverding, 2009), and p67, a lysosomal membrane glycoprotein (Kelley *et al*., 1999; Alexander *et al*., 2002), as endogenous reporters. As previously noted in pulse-chase analyses of control cells (Tazeh *et al*., 2009), TbCatL was synthesized as an initial 53 kDa proprotein and an additional 50 kDa precursor 'X', both of which were converted over time to a 44 kDa active form, indicating lysosomal arrival (Fig. 8A, top). Precursor X is derived from the full-length TbCatL orf (Tazeh *et al*., 2009), and may represent alternate translational initiation and/or post-translational processing. TbRab7 silencing did not alter the pattern (Fig. 8A, top) or rate (Fig. 8A, bottom) of processing to the mature 44 kDa lysosomal form. Like TbCatL, p67 is cleaved upon arrival in the lysosome from a 100 kDa ER glycoform (gp100), via a 150 kDa Golgi intermediate (gp150), to quasi-stable fragments (gp42, gp32), the appearance of which can be used as kinetic indicators of arrival in the lysosome (Fig. 8B, top) (Alexander *et al*., 2002). Quantitative analyses of these events demonstrate that TbRab7 silencing does not affect either the extent or kinetics of p67 processing (Fig. 8B, bottom). Collectively, these surprising results compellingly demonstrate that TbRab7 is not required for biosynthetic trafficking of endogenous soluble or membrane lysosomal proteins in BSF trypanosomes.

TbRab7 and default lysosomal trafficking

To determine the effect of TbRab7 silencing on the default trafficking pathway to the lysosome in BSF trypanosomes, we used engineered soluble and membrane-bound default reporters whose native full-length counterparts normally traffic to the cell surface (VSG) or to the lysosome (p67). We first performed pulse-chase analysis on VSG117ΔGPI (deletion of C-terminal GPI attachment signal, soluble). As previously reported (Triggs and Bangs, 2003), cell-associated VSG117ΔGPI in control cells decreased over time with minimal secretion into the medium (Fig. 9A, top), and this loss was quantitatively reversed by the lysosomal cysteine protease inhibitor FMK024 (Fig. 9A, bottom), a hallmark of lysosomal delivery. TbRab7 silencing altered neither the rate or extent of degradation, nor the recovery of cell-associated VSGΔGPI after FMK024 treatment, indicating no defect in lysosomal trafficking of this reporter. We next performed similar analyses on the p67-derived default reporters p67ΔTM (Fig. 9B, deletion of C-terminal transmembrane & cytoplasmic domains, soluble) and p67ΔCD (Fig. 9C, deletion of C-terminal cytoplasmic domain alone, membrane-bound). Delivery of these reporters to the lysosome can be followed by the loss of the initial gp100 ER glycoform and/or the production of the standard set of quasi-stable p67 fragments (gp42 & gp32). For each reporter, initial gp100 disappeared over time but was fully recovered with FMK024 treatment (top panels). In addition, the typical fragmentation pattern was seen with membrane-bound p67ΔCD. Again, no differences in either the rate or extent of turnover for either reporter was seen in control vs. TbRab7

silenced cells (bottom panels). These results clearly demonstrate that TbRab7 silencing does not affect lysosomal delivery of default trafficking reporters.

Discussion

We present here the first functional study of Rab7 in trypanosomes. Consistent with Engstler *et al*. (2004), we find the TbRab7^{+} late endosome to be a discrete compartment in close juxtaposition to the terminal p67^{+} lysosome. Contrary to published claims (Field and Carrington, 2009), we see no significant overlap of these two compartmental markers. Not surprisingly given the high rate of endocytosis and the importance of lysosomal function (Langreth and Balber, 1975; Coppens *et al*., 1987; Engstler *et al*., 2004; Peck *et al*., 2008), depletion of TbRab7 is lethal in BSF trypanosomes. In stark contrast, TbRab7 is apparently non-essential in PCF trypanosomes where the rate of endocytosis and the importance of lysosomal activities are much lower. Cultured PCF trypanosomes were fully viable under both RNAi silencing and conditional knockout of TbRab7, and in the latter case specific mRNA was reduced below the limits of detection. However, repeated attempts (n = 6) to obtain an unconditional double knockout in PCF cells were unsuccessful (data not shown) suggesting to the contrary that TbRab7 may be essential. Perhaps sufficient TbRab7 remains after both prolonged knockdown and conditional knockout to support the minimal function required for viability. Alternatively, the gradual loss of protein in these situations may allow for adaptation to life without TbRab7, whereas the catastrophic loss in a traditional double knockout is too severe for cells to survive drug selection. Whatever the explanation, our results indicate at the least that much less TbRab7 is required for growth of PCF trypanosomes.

In both mammals and yeast, Rab7 (Ypt7p in yeast) regulates delivery of endocytic cargo to the lysosome (Wichmann *et al*., 1992; Schimmoller and Riezman, 1993; Bucci *et al*., 2000; Vanlandingham and Ceresa, 2009). In each system, disruption of Rab7 function can lead to lysosomal disruption/dispersal (Wichmann *et al*., 1992; Bucci *et al*., 2000). Likewise, we show here in BSF trypanosomes that TbRab7 regulates lysosomal delivery of endocytic cargo, and that this sorting takes place in the late endosome. However, in this case lysosomal morphology is unaffected by TbRab7 ablation. Consistent with endosomal arrest, both endocytosed TL and TLF in TbRab7 silenced cells accumulated in a pre-lysosomal compartment with an acidic but elevated internal pH. This likely represents disrupted late endosomes, but a lack of suitable markers besides TbRab7 itself precludes definitive identification. Alternatively, as trafficking from the early and recycling endosomes to the lysosome is clathrin-dependent (Engstler *et al*., 2004), this may represent accumulation of undocked transport vesicles. Loss of TbRab7 had other subtle effects on endosomal function. There was no impact on the initial rate of TL uptake, indicating that clathrin-mediated endocytosis at the flagellar pocket is normal. However, both total binding and uptake were significantly reduced, correlating with a specific reduction in surface TfR, a GPI-anchored pNAL-bearing flagellar pocket receptor. Interestingly, binding/uptake of TLF was normal in TbRab7 depleted cells, suggesting that surface levels of HpHbR (TLF receptor), another GPI-anchored pNAL-bearing flagellar pocket protein (Vanhollebeke *et al*., 2008), were unaffected. TLF binding/uptake assays performed at tenfold ligand excess (50 μg ml^{-1}) were also unimpaired, minimizing the possibility that sub-saturating levels of

ligand were obscuring a reduction of this receptor (data not shown). Thus reduced endocytosis of TL is not due to global effects on pNAL synthesis (confirmed by lectin blotting); rather it appears to result from selective reduction of specific flagellar pocket constituents. Presumably the difference between TfR and HpHbR relate to differences in how these proteins transit the endosomal compartments. Internalized VSG recycles in part through the late endosome (Engstler *et al*., 2004), and this may be true also for TfR leading to depletion of the surface pool in TbRab7 silenced cells. HpHbR recycling on the other hand may avoid the late endosome and consequently is unaffected. An interesting sidelight to these experiments is that blocking transport to the lysosome dramatically reduces the trypanocidal activity of TLF. TLF activity is dependent on normal lysosomal physiology, and temperature block experiments suggest that lysosomal delivery is essential (Hager *et al*., 1994; Peck *et al*., 2008), but this is the first unambiguous proof that delivery to the lysosome is a prerequisite for optimal activity.

In both mammals and yeast, Rab7 also regulates trafficking of biosynthetic cargo to the lysosome (Wichmann *et al*., 1992; Rojas *et al*., 2008), including cathepsin D in mammals and alkaline phosphatase and carboxypeptidase Y in yeast, but surprisingly this is not the case in trypanosomes. Maturation of p67 and TbCatL, both of which require proteolysis in the lysosome, were unaffected by TbRab7 silencing. It is possible that enough TbRab7 remains following knockdown to fully support this pathway, but the dramatic effect of silencing on endocytic trafficking strongly argues against this possibility. Although an unexpected result, this does not necessarily mean that biosynthetic cargo to the lysosome bypasses the late endosome. It may be that entry of endocytic cargo from the early and recycling endosomes into the late endosome are TbRab7 restricted, but some other Rab, perhaps TbRab4, which has been loosely implicated in post-Golgi trafficking (Hall *et al*., 2004), regulates entry from the Golgi. A similar argument could be made for selective regulation of cargo exit from the late endosome *en route* to the lysosome, although this seems less probable because at this point all cargo are likely to be treated the same regardless of origin. Alternatively, it may be that biosynthetic cargo does completely bypass the late endosome in trypanosomes, a possibility that is discussed below. Whatever the case, this striking result reveals that post-Golgi trafficking to the lysosome in trypanosomes is fundamentally distinct from other eukaryotic systems.

Another unexpected outcome of this work is that trafficking of default lysosomal reporters is also TbRab7-independent. We previously hypothesized that these reporters leave the Golgi with normal secretory cargo and intersect the endocytic pathway to be swept back to the lysosome (Tazeh *et al*., 2009). This work is the first step in challenging our proposal, and the results seemingly contradict the original hypothesis. Again this does not mean that default cargo bypasses the endocytic compartment entirely. But at the least, the tight blockade of normal endocytic trafficking without affecting default trafficking strongly suggests that these reporters do not transit the late endosome in the same manner as bona fide endocytic cargo. Nevertheless, it is possible that default cargo still intersects the endocytic pathway and then passes directly from the early and/or recycling endosomes to the lysosome, as has been suggested for fluid phase cargo (Engstler *et al*., 2004), but it is difficult to see how such a pathway could be so exclusive as to be totally unaffected by Rab7

knockdown. Furthermore, one default reporter, p67ΔCD, is membrane-bound and is difficult to accommodate by such a model. Alternatively, it is possible that default cargo does not utilize the endocytic pathway at all, instead proceeding directly from the Golgi to the lysosome, and this has implications for how biosynthetic cargo accesses the lysosome under TbRab7 knockdown. Perhaps biosynthetic cargo does normally transit the late endosome in a TbRab7-dependent manner, but is rerouted through the default pathway when the endosomal route is blocked. Whatever the nature of the post-Golgi default pathway, we can now confirm two features – it is independent of normal AP-1/clathrin mediated exit from the Golgi (Tazeh *et al*., 2009), and it does not require normal TbRab7 function in the late endosome (this work). Only further analyses of the role of the other endosomal Rabs, and perhaps other components of vesicular trafficking, in BSF trypanosomes will illuminate these issues.

Finally in this regard, it is worth commenting on the related issue of multi-vesicular bodies (MVBs) in trypanosomes. In mammalian systems MVBs are pre-lysosomal compartments that sort certain classes of endocytic cargo to the lysosome, including ubiquitinylated membrane proteins (Wollert and Hurley, 2010). Morphologically MVBs are large discrete vacuoles with internal vesicles. They typically contain Rab7 and are often considered as synonymous with late endosomes (Vanlandingham and Ceresa, 2009). MVBs also typically contain components of the ESCRT machinery for internal vesiculation and lysosomal targeting of ubiquitinylated proteins (Wollert and Hurley, 2010), and retromer machinery for retrieval of membrane components to the Golgi (Rojas *et al*., 2008). The term MVB has been used to loosely describe miscellaneous cytological features in trypanosomes for many years (Vickerman, 1969; Langreth and Balber, 1975), and aberrant MVB-like structures have been observed in stressed cells following RNAi silencing of the AP-1 γ subunit (Allen *et al*., 2007) and p67 (Peck *et al*., 2008), the latter example being derived from the terminal lysosome. However, unlike the typical p67-positive lysosome and the various TbRab-positive endosomes, and contrary to published claims (Leung *et al*., 2008; Field and Carrington, 2009), no consistent morphological MVB structure with validated markers has ever been defined in normal trypanosomes. Nevertheless, orthologues of the ESCRT and retromer machinery have been identified, and at least in the case of TbESCRT proteins have been shown to carry out expected functions (Leung *et al*., 2008; Koumandou *et al*., 2011). When visualized both ESCRT and retromer orthologues were found to have locations consistent with that seen here for the late endosome, although formal colocalization with TbRab7 was not made. Resolution of this issue will require additional imaging studies, but if the ESCRT and retromer machinery do colocalize with TbRab7, it will indicate that the functions typically associated with MVBs are carried out by the late endosome in trypanosomes. And if this is true, it may provide new avenues for investigating the regulation of both biosynthetic and default trafficking to the lysosome.

Experimental procedures

Parasite cultures

Bloodstream form and PCF Lister 427 *T. brucei brucei* were grown in HMI-9 and Cunningham's media, as previously described (Tazeh and Bangs, 2007; Peck *et al*., 2008).

Tetracycline-responsive 29–13 PCF and single-marker BSF cell lines (Wirtz *et al*., 1999) used for inducible expression experiments were maintained in the same media supplemented with tet-free serum (Atlanta Biologicals, Lawrenceville, GA, USA).

Molecular constructs and transfection

All TbRab7 constructs created here are derived from *T. b. brucei* gene Tb09.211.2330 (http://tritrypdb.org), which is annotated as a Rab7 orthologue. A second putative Rab7 gene, Trab7 (Tb927.8.4620), has been re-annotated as a Rab31 orthologue and is not considered in this work (Field *et al*., 2000).

A TbRab7 stem-loop RNAi construct was generated using pLEW100.v5 (http://tryps.rockefeller.edu/). First, an overhanging double-stranded oligonucleotide (containing 5′-3′: HindIII, XhoI, XbaI and BamHI restriction sites) was ligated into HindIII/BamHI restricted plasmid to generate pLEW100. v5X. Second, a 477 bp Pex11 stuffer fragment (Tazeh *et al*., 2009) was inserted using flanking 5′ XhoI and 3′ XbaI sites to generate the pLEW100v5X:Pex11 stem loop vector. This fragment has internal and penultimate 5′ AscI and 3′ NdeI sites. Third, a 450 bp region (nts 214–658) of the TbRab7 orf (Tb09.211.2330), chosen using RNAit (Redmond *et al*., 2003), was PCR amplified with 5′ XbaI/XhoI and 3′ AscI/NdeI sites. This was then sequentially inserted upstream of the Pex11 stuffer using XhoI/AscI, and then downstream in the opposite orientation using XbaI/NdeI. The resultant plasmid was linearized with NotI for transfection.

An *in situ* TbRab7 N-terminal Ty tagging construct was prepared using pXS6^{neo}, a version of pXS5 (Alexander *et al*., 2002) with the XhoI linearization site replaced with NotI. First, the full β-α tubulin intergenic region (Sather and Agabian, 1985) was PCR amplified from genomic DNA with flanking 5′ PacI and 3′ XhoI/SacI sites and used to replace the partial β-α tubulin intergenic region in pXS6. The TbRab7 ORF was then PCF amplified (nts 3–525) with an N-terminal in-frame fusion of a Ty epitope tag (MEVHTNQDPLD, Ty underlined) (Bastin *et al*., 1996), and with flanking 5′ XhoI and 3′ SacI sites, and inserted into the corresponding sites of the tagging construct. Next, the TbRab7 5′ intergenic region (nts −1 to −500 relative to the TbRab7 start codon) was amplified with flanking 5′ HindIII and 3′ EcoRI sites and inserted into the construct. The completed tagging construct, consisting of (5′ to 3′) the TbRab7 5′ intergenic region, the aldolase intergenic region, the *neo*^{r} cassette, the β-α tubulin intergenic region, and the N-terminal Ty tagged TbRab7 orf, was excised with HindIII/SacI for transfection.

A TbRab7 conditional knockout cell line was created using pyrFEKO-PUR and pyrFEKO-BSD (http://tryps.rockefeller.edu/). Into each vector, the TbRab7 5′ UTR (nts −455 to +70 relative to the TbRab7 start codon) was PCF amplified and inserted using flanking 5′ PvuII and 3′ HindIII sites. The 3′ UTR (nts 1–453 relative to the TbRab7 stop codon) was similarly amplified and inserted using 5′ BamHI and 3′ SbfI sites. This generated matched knockout constructs with a puromycin or blasticidin resistance cassette between the TbRab7 UTRs. To generate the TbRab7 conditional knockout cell line, the pyrFEKO-PUR: :TbRab7 construct was first excised by PvuII/SbfI digestion and transfected into 29–13 PCF cells to generate a single knockout cell line. Second, a tet-inducible TbRab7 construct was created using pLew100X (created from pLew100 as described above for pLew100v5X). The entire

TbRab7 ORF was PCR amplified and inserted into pLew100X using flanking 5′ XhoI and 3′ XbaI sites. This construct was then linearized with NotI and transfected into the single knockout cell line. Third, while maintaining cells in the presence of tetracycline, the PvuII/SbfI excised pyrFEKO-BSD:TbRab7 construct was transfected into the single knockout/inducible TbRab7 cell line to generate the final conditional TbRab7 double knockout line. Conditional TbRab7 expression in these cells was terminated by extensive washing and culturing in tet-free media. Replacement of the native TbRab7 alleles was confirmed by PCR amplification of the TbRab7 locus with flanking primers (nt −90 to −70 upstream and 1 to 18 downstream of the TbRab7 orf) (Fig. 3).

The p67ΔTM and p67ΔCD default trafficking reporters (Alexander *et al*., 2002) were recreated with in-frame C-terminal 3x HA tags (1x: YPYDVPDYA). Briefly, codons 1–616 (p67ΔTM) and 1–639 (p67ΔCD) of the p67 open reading frame (Tb927.5.1810) were PCR amplified from genomic DNA with flanking 5′ HindIII and 3′ XhoI sites and inserted into the same sites in the constitutive expression vector pXS6^{pur}:HA3x (details available on request). These constructs were linearized with NotI for transfection. Likewise the default trafficking reporter VSG117ΔGPI (Triggs and Bangs, 2003), in the constitutive expression vector pXS5^{pur} (Sevova and Bangs, 2009), was linearized with XhoI for transfection.

All constructs were sequence verified. Linearized plasmids and excised constructs were introduced into the appropriate host cells by electroporation as described previously (Burkard *et al*., 2007; Sevova and Bangs, 2009), and clonal cell lines were derived by limiting dilution and selection with the appropriate antibiotic. Induction of TbRab7 dsRNA and conditional expression of TbRab7 was achieved with 1 μg ml^{-1} of tetracycline.

Antibody, secondary and blotting reagents

Rabbit anti-VSG117 and anti-VSG221, rabbit anti-TbCatL, rabbit anti-BiP, and mouse monoclonal anti-p67 have been described elsewhere (McDowell *et al*., 1998; Peck *et al*., 2008). The anti-VSG117 was negatively selected on VSG221-sepharose to eliminate cross-reaction with the endogenous VSG221 (Triggs and Bangs, 2003). Rat anti-Rab7 was the kind gift of Dr Markus Engstler (University of Wuerzburg) and rabbit anti-transferrin receptor (TfR) was the generous gift of Drs Piet Borst and Henri van Luenen (The Netherlands Cancer Institute, Amsterdam). Mouse anti-Ty was from the UAB Hybridoma Facility (Birmingham, AL, USA) and rabbit anti-HA was from Sigma-Aldrich (St Louis, MO, USA). Alexa Fluor-conjugated goat secondary antibodies were purchased from Molecular Probes (Eugene, OR, USA). The following ligand conjugates were used for endocytosis assays: transferrin:Alexa Fluor 488 (Tf:A488, Molecular Probes); tomato lectin:biotin and tomato lectin:fluorescein (TL:Bio & TL:FITC, Vector Laboratories, Burlingame, CA, USA); and tomato lectin:Alexa Fluor 488 [TL:488, prepared as in Tazeh *et al*. (2009)]. Streptavidin:Alexa Fluor 488 (SA:A488, Molecular Probes) was used for secondary detection of TL:Bio. Horseradish peroxidase (HRP)-conjugated streptavidin (SA) and anti-rabbit IgG were from KPL (Gaithersburg, MD, USA).

Radiolabelling and immunoprecipitation

Pulse-chase metabolic radiolabelling with [^{35}S]Met/Cys (Perkin Elmer, Waltham, MA, USA) and subsequent immunoprecipitation of specific radiolabelled proteins from cell lysates were performed as described previously (Alexander *et al*., 2002). For BSF cells, pulse times were 15 min for p67 trafficking and 10 min for TbCatL and VSG117ΔGPI trafficking. Immunoprecipitations were fractionated by SDS-PAGE and dried gels were analysed by phosphorimaging using a Typhoon FLA 9000 with native ImageQuant Software (GE Healthcare, Piscataway, NJ, USA). Bands were quantified by volume analysis on areas of interest after subtracting background signal from unlabeled areas.

Surface biotinylation

Biotinylation of surface proteins was performed as previously described (Gruszynski *et al*., 2003). Cells on ice were treated (10^8 cells ml^{-1}, 30 min) with Sulfo-NHS-Biotin (400 μg ml^{-1}, Thermo Fisher Scientific, Rockford, IL, USA). The reaction was quenched by diluting to 10^7 cells ml^{-1} with PBSG containing NH_4Cl (10 mM final). Cells were washed in PBS with glucose (10 mg ml^{-1}) and processed for immunoprecipitation as described above. Streptavidin blotting of immunoprecipitated proteins was then performed as described below.

Protein and Northern analyses

For protein blotting whole cell lysates or immunoprecipitates were fractioned by SDS-PAGE, transferred using an Owl semi dry apparatus (Thermo Fisher Scientific) to an Immobilon-P transfer membrane (Millipore, Bedford, MA, USA), and blocked in a 5% milk solution. For whole cell blots, membranes were incubated 1 h with anti-TfR (1/5 000) or TL:Bio (1 μg ml^{-1}), washed, and incubated with anti-rabbit IgG:HRP or SA:HRP (1/10 000, 1 h). For blots of biotinylated immunoprecipitates membranes were incubated directly with SA:HRP. In each case the final washed blots were visualized on X-ray film using Pierce SuperSignal West Pico substrate (Thermo Fisher Scientific), as described elsewhere in more detail (Gruszynski *et al*., 2003).

For Northern analysis, total RNA was extracted from mid-log phase *T. brucei*, fractionated on agarose/formaldehyde gels, transferred to a Zeta Probe nylon membrane (Bio-Rad Laboratories, Hercules, CA, USA), and probed as previously described (Sevova and Bangs, 2009; Tazeh *et al*., 2009). mRNAs of interest were detected using [^{32}P]dCTP-labelled DNA probes. Blots were probed first for TbRab7 (nts 214–658) and, after subsequent stripping, reprobed for β-tubulin as a loading control. Hybridization was analysed by phosphorimaging as described above for immunoprecipitations.

Epifluorescence microscopy

For IFA microscopy cells were methanol/acetone-fixed as previously described (Peck *et al*., 2008). Cells were stained with primary and secondary antibodies diluted in blocking buffer and mounted as described in Sevova and Bangs (2009). Cells were also stained with DAPI (0.5 μg ml^{-1}) to reveal nuclei and kinetoplasts. Serial image stacks (0.2 micron Z-increment) were collected with capture times from 100–500 ms (100x PlanApo, oil immersion, 1.4 na)

on a motorized Zeiss Axioplan IIi equipped with a rear-mounted excitation filter wheel, a triple pass (DAPI/FITC/Texas Red) emission cube, differential interference contrast optics, and an Orca AG CCD camera (Hamamatsu, Bridgewater, NJ, USA). All images were collected with OpenLabs 5.0 software (Improvision, Lexington, MA, USA) and individual channel stacks were deconvolved by a constrained iterative algorithm, pseudocolored and merged using Volocity 5.0 software (Improvision). All images presented are summed stack projections of individual or merged channels. The xyz pixel precision of this arrangement has been validated in Sevova and Bangs (2009) (Fig. S1 therein).

For flow cytometric assays of endocytosis, labelled cells (see below) were analysed on a LSR II instrument (BD Biosciences, San Jose, CA, USA) using native FACSDiva acquisition software and FlowJo analysis software (Tree Star, Ashland, OR, USA), collecting 10 000 events per data point, as previously described (Tazeh *et al*., 2009). For internal pH determination with TL:FITC cells were analysed live with DAPI (5 μg ml^{-1}) staining to exclude dead cells during acquisition. For all other endocytic ligands cells were fixed (2% formaldehyde) before flow analysis.

Endocytosis assays

Standard binding and uptake assays have been previously described (Tazeh *et al*., 2009). Briefly, for binding washed cells (10^7 ml^{-1}) were incubated (30 min, 5°C) with TL (5 μg ml^{-1}) in serum-free HMI9 with 0.5 mg ml^{-1} BSA. For uptake experiments cells were incubated with TL for 30 min at 37°C, washed and then incubated in fresh media for 20 min to chase ligand into the terminal lysosome. For TL:FITC pulse chase uptake cells were labelled under binding conditions, washed into fresh binding medium, and incubated at 37°C to chase bound ligand into internal compartments. In each case cells were processed for IFA or flow cytometry as described above, and TL:Bio was detected using SA:488.

TL uptake and electron microscopy

Log phase TbRab7 RNAi cells (4×10^7) were washed and resuspended in serum-free HMI9 with 0.5 mg ml^{-1} BSA (0.78 ml). TL:colloidal gold (0.22 ml in PBS, OD_{520} ~ 4, 15 nm, EY Laboratories, San Mateo, CA, USA) was added to give a final TL concentration of ~ 4 μg ml^{-1} and the cells were incubated at 37°C (2 h) to allow uptake. Cells were then washed and resuspended at 10^5 ml^{-1} in complete HMI9 medium, and equal portions were cultured for 28 h with or without tetracycline (1 μg ml^{-1}). Cells were harvested by centrifugation, washed in PBS, and then fixed overnight (4°C) in 2.5% glutaraldehyde, 2.0% para-formaldehyde in 0.1 M sodium cacodylate buffer, pH 7.4. The cells were post-fixed in 1% osmium tetroxide in the same buffer for 1 h at RT. Samples were then serially dehydrated in ethanol, transferred into propylene oxide and flat-embedded in Spurr's epoxy resin (Electron Microscopy Sciences, Hatfield, PA, USA). Sections (60–90 nm) were cut on a Reichert-Jung Ultracut-E Ultramicrotome and contrasted with uranyl acetate in 50% EtOH. Ultrathin sections were mounted and observed with a Philips CM120 electron microscope. All images were captured with a MegaView III (Soft ImagingSystem; Lakewood, CO, USA) side-mounted digital camera.

TLF assays

Purified trypanolytic facter-1 (TLF) and Alexa Fluor 488-conjugated TLF (TLF:A488) were produced as previously described (Kieft *et al*., 2010). TLF:A488 fluorescence microscopy and flow cytometry experiments were performed as described above using 5.0 μg ml^{-1} in serum-complete HMI-9 medium. Lysis assays were performed with unconjugated TLF (0.8 μg ml^{-1}) in serum-complete HMI-9 as previously described (Peck *et al*., 2008; Kieft *et al*., 2010).

Statistical analyses

Curve fitting (linear regression) and statistical analyses were performed with Prism 4 software (GraphPad Software, San Diego CA, USA). Biological replicates (*n*) are indicated.

Supplementary Material

Refer to Web version on PubMed Central for supplementary material.

Acknowledgments

The authors are grateful to Bangs lab members past and present who have contributed in many ways to this work, including Dr Ngii Tazeh, and Dr Eli Theel (née Sevova). We also thank Drs Piet Borst and Henri van Luenen (The Netherlands Cancer Institute, Amsterdam) for generous supplies of anti-TfR antibody, Dr Markus Engstler (Biocenter of the University of Würzburg, Germany) for anti-TbRab7 antibody, and Dr George Cross (Rockefeller University, NY) for pLew100, pLew100.v5 and the pyrFEKO vectors. This work supported by United States Public Health Service Grants R01 AI35739 and R01 AI056866 to J.D.B., and R01 AI39033 to S.L.H. J.S.S. was supported by NIH 'Cellular and Molecular Parasitology' Training Grant (T32 AI07414) to UW-Madison.

References

Alexander DL, Schwartz KJ, Balber AE, Bangs JD. Developmentally regulated trafficking of the lysosomal membrane protein p67 in *Trypanosoma brucei*. J Cell Sci. 2002; 115:3253–3263. [PubMed: 12140257]

Allen CL, Goulding D, Field MC. Clathrin-mediated endocytosis is essential in *Trypanosoma brucei*. EMBO J. 2003; 22:4991–5002. [PubMed: 14517238]

Allen CL, Liao D, Chung WL, Field MC. Dileucine signal-dependent and AP-1-independent targeting of a lysosomal glycoprotein in *Trypanosoma brucei*. Mol Biochem Parasitol. 2007; 156:175–190. [PubMed: 17869353]

Aslett M, Aurrecoechea C, Berriman M, Brestelli J, Brunk BP, Carrington M, et al. TriTrypDB: a functional genomic resource for the Trypanosomatidae. Nucleic Acids Res. 2010; 38:D457–D462. [PubMed: 19843604]

Balber AE, Bangs JD, Jones SM, Proia RL. Inactivation or elimination of potentially trypanolytic, complement-activating immune complexes by pathogenic trypanosomes. Infect Immun. 1979; 24:617–627. [PubMed: 468370]

Barry JD. Capping of variable antigen on *Trypanosoma brucei*, and its immunological and biological significance. J Cell Sci. 1979; 37:287–302. [PubMed: 383734]

Bastin P, Bagherzadeh Z, Matthews KR, Gull K. A novel epitope tag system to study protein targeting and organelle biogenesis in *Trypanosoma brucei*. Mol Biochem Parasitol. 1996; 77:235–239. [PubMed: 8813669]

Biebinger S, Helfert S, Steverding D, Ansorge I, Clayton C. Impaired dimerization and trafficking of ESAG6 lacking a glycosyl-phosphatidylinositol anchor. Mol Biochem Parasitol. 2003; 132:93–96. [PubMed: 14599669]

Böhme U, Cross GA. Mutational analysis of the variant surface glycoprotein GPI-anchor signal sequence in *Trypanosoma brucei*. J Cell Sci. 2002; 115:805–816. [PubMed: 11865036]

Braulke T, Bonifacino JS. Sorting of lysosomal proteins. Biochim Biophys Acta. 2009; 1793:605–614. [PubMed: 19046998]

Bucci C, Thomsen P, Nicoziani P, McCarthy J, van Deurs B. Rab7: a key to lysosome biogenesis. Mol Biol Cell. 2000; 11:467–480. [PubMed: 10679007]

Burkard G, Fragoso CM, Roditi I. Highly efficient stable transformation of bloodstream forms of *Trypanosoma brucei*. Mol Biochem Parasitol. 2007; 153:220–223. [PubMed: 17408766]

Caffrey CR, Steverding D. Kinetoplastid papain-like cysteine peptidases. Mol Biochem Parasitol. 2009; 167:12–19. [PubMed: 19409421]

Coppens I, Opperdoes FR, Courtoy PJ, Baudhuin P. Receptor-mediated endocytosis in the bloodstream form of *Trypanosoma brucei*. J Protozool. 1987; 34:465–473. [PubMed: 2828605]

Drain J, Bishop JR, Hajduk SL. Haptoglobin-related protein mediates trypanosome lytic factor binding to trypanosomes. J Biol Chem. 2001; 276:30254–30260. [PubMed: 11352898]

Engstler M, Thilo L, Weise F, Grunfelder CG, Schwarz H, Boshart M, Overath P. Kinetics of endocytosis and recycling of the GPI-anchored variant surface glycoprotein in *Trypanosoma brucei*. J Cell Sci. 2004; 117:1105–1115. [PubMed: 14996937]

Engstler, M.; Bangs, JD.; Field, MC. Intracellular transport systems in trypanosomes: function, evolution and virulence. In: Barry, JD.; Mottram, JC.; McCulloch, R.; Acosta-Serrano, A., editors. Trypanosomes – After the Genome. Wymondham, UK: Horizon Scientific Press; 2006. p. 281-317.

Field H, Sherwin T, Smith AC, Gull K, Field MC. Cell-cycle and develpmental regulation of TbRAB31 localisation, a GTP-locked Rab protein from *Trypanosoma brucei*. Mol Biochem Parasitol. 2000; 106:21–35. [PubMed: 10743608]

Field MC, Carrington M. The trypanosome flagellar pocket. Nat Rev Microbiol. 2009; 7:775–786. [PubMed: 19806154]

Grosshans BL, Ortiz D, Novick P. Rabs and their effectors: achieving specificity in membrane traffick. Proc Natl Acad Sci. 2006; 103:11821–11827. [PubMed: 16882731]

Grünfelder CG, Engstler M, Wieise F, Schwarz H, Stierhof Y-D, Morgan GW, et al. Endocytosis of a glycosylphosphatidylinositol-anchored protein via clatherin-coated vesicles, sorting by default in endosomes and exocytosis via RAB11-positive carriers. Mol Biol Cell. 2003; 14:2029–2040. [PubMed: 12802073]

Gruszynski AE, DeMaster A, Hooper NM, Bangs JD. Surface coat remodeling during differentiation of *Trypanosoma brucei*. J Biol Chem. 2003; 278:24665–24672. [PubMed: 12716904]

Hager KM, Pierce MA, Moore DR, Tytler EM, Esko JD, Hajduk SL. Endocytosis of a cytotoxic human high density lipoprotein results in disruption of acidic intracellular vesicles and subsequent killing of African trypanosomes. J Cell Biol. 1994; 126:155–167. [PubMed: 8027174]

Hajduk SL, Moore DR, Vasudevacharya J, Siqueira H, Torri AF, Tytler EM, Esko JD. Lysis of *Trypanosoma brucei* by a toxic subspecies of human high density lipoprotein. J Biol Chem. 1989; 264:5210–5217. [PubMed: 2494183]

Hall BS, Pal A, Goulding D, Field MC. Rab4 is an essential regulator of lysosomal trafficking in trypanosomes. J Biol Chem. 2004; 279:45047–45056. [PubMed: 15284229]

Hall BS, Smith E, Langer W, Jacobs LA, Goulding D, Field MC. Developmental variation in Rab11-dependent trafficking in *Trypanosoma brucei*. Eukaryot Cell. 2005; 4:971–980. [PubMed: 15879531]

Huete-Perez JA, Engel JC, Brinen JC, Mottram JC, McKerrow JH. Protease trafficking in two primitive eukaryotes is mediated by a prodomain protein motif. J Biol Chem. 1999; 274:16249–16256. [PubMed: 10347181]

Kelley RJ, Alexander DL, Cowan C, Balber AE, Bangs JD. Molecular cloning of p67, a lysosomal membrane glycoprotein from *Trypanosoma brucei*. Mol Biochem Parasitol. 1999; 98:17–28. [PubMed: 10029306]

Kieft R, Capewell P, Turner CM, Veitch NJ, MacLeod A, Hajduk S. Mechanism of *Trypanosoma brucei gambiense* (group 1) resistance to human trypanosome lytic factor. Proc Natl Acad Sci. 2010; 107:16137–16141. [PubMed: 20805508]

Koumandou VL, Klute MJ, Herman EK, Nunez-Miguel R, Dacks JB, Field MC. Evolutionary reconstruction of the retromer complex and its function in *Trypanosoma brucei*. J Cell Sci. 2011; 124:1496–1509. [PubMed: 21502137]

Langreth SG, Balber AE. Protein uptake and digestion in bloodstream and culture forms of *Trypanosoma brucei*. J Protozool. 1975; 22:40–53. [PubMed: 1117436]

Leung KF, Dacks JB, Field MC. Evolution of the multivesicular body ESCRT machinery; retention across the eukaryotic lineage. Traffic. 2008; 9:1698–1716. [PubMed: 18637903]

Ligtenberg MJ, Bitter W, Kieft R, Steverding D, Janssen H, Calafat J, Borst P. Reconstitution of a surface transferrin binding complex in insect form *Trypanosoma brucei*. EMBO J. 1994; 13:2565–2573. [PubMed: 8013456]

McCann AK, Schwartz KJ, Bangs JD. A determination of the steady state lysosomal pH of bloodstream stage African trypanosomes. Mol Biochem Parasitol. 2008; 159:146–149. [PubMed: 18359105]

McDowell MA, Ransom DM, Bangs JD. Glycosylphosphatidylinositol-dependent secretory transport in *Trypanosoma brucei*. Biochem J. 1998; 335:681–689. [PubMed: 9794811]

Morgan GW, Allen CL, Jeffries TR, Hollinshead M, Field MC. Developmental and morphological regulation of clathrin-mediated endocytosis in *Trypanosoma brucei*. J Cell Sci. 2001; 114:2605–2015. [PubMed: 11683388]

Nolan DP, Geuskens M, Pays E. N-linked glycans containing linear poly-N-acetyllactosamine as sorting signals in endocytosis in *Trypanosoma brucei*. Curr Biol. 1999; 9:1169–1172. [PubMed: 10531030]

Pal A, Hall BS, Nesbeth DN, Field HI, Field MC. Differential endocytic functions of *Trypanosoma brucei* Rab5 isoforms reveal a glycosylphosphatidylinositol-specific endosomal pathway. J Biol Chem. 2002; 277:9529–9539. [PubMed: 11751913]

Pal A, Hall BS, Jefferies TR, Field MC. Rab5 and Rab11 mediate transferrin and anti-variant surface glycoprotein recycling in *Trypanosoma brucei*. Biochem J. 2003; 374:443–451. [PubMed: 12744719]

Pamer EG, So M, Davis CE. Identification of a developmentally regulated cysteine protease of *Trypanosoma brucei*. Mol Biochem Parasitol. 1989; 33:27–32. [PubMed: 2710163]

Peck RF, Shiflett AM, Schwartz KJ, McCann A, Hajduk SL, Bangs JD. The LAMP-like protein p67 plays an essential role in the lysosome of African trypanosomes. Mol Microbiol. 2008; 68:933–946. [PubMed: 18430083]

Poole B, Ohkuma S. Effect of weak bases on the intralysosomal pH in mouse peritoneal macrophages. J Cell Biol. 1981; 90:665–669. [PubMed: 6169733]

Redmond S, Vadivelu J, Field MC. RNAit: an automated web-based tool for the selection of RNAi targets in *Trypanosoma brucei*. Mol Biochem Parasitol. 2003; 128:115–118. [PubMed: 12706807]

Rifkin MR. *Trypanosoma brucei*: new radioisotope assay for quantitating cell lysis. Exp Parasitol. 1978; 46:207–212. [PubMed: 729697]

Rojas R, van Vlijmen T, Mardones GA, Prabhu Y, Rojas AL, Mohammed S, et al. Regulation of retromer recruitment to endosomes by sequential action of Rab5 and Rab7. J Cell Biol. 2008; 183:513–526. [PubMed: 18981234]

Saftig P, Klumperman J. Lysosome biogenesis and lysosomal membrane proteins: trafficking meets function. Nat Rev Mol Cell Biol. 2009; 10:623–635. [PubMed: 19672277]

Sather S, Agabian N. A 5′ spliced leader is added in trans to both alpha- and beta-tubulin transcripts in *Trypanosoma brucei*. Proc Natl Acad Sci. 1985; 82:5695–5699. [PubMed: 2994042]

Schimmoller F, Riezman H. Involvement of Ypt7p, a small GTPase, in traffic from late endosome to the vacuole in yeast. J Cell Sci. 1993; 106:823–830. [PubMed: 8308065]

Schwartz KJ, Peck RF, Tazeh NN, Bangs JD. GPI valence and the fate of secretory membrane proteins in African trypanosomes. J Cell Sci. 2005; 118:5499–5511. [PubMed: 16291721]

Schwede A, Carrington M. Bloodstream form trypanosome plasma membrane proteins: antigenic variation and invariant antigens. Parasitology. 2010; 137:2029–2039. [PubMed: 20109254]

Seabra MC, Wasmeier C. Controlling the location and activation of Rab GTPases. Curr Opin Cell Biol. 2004; 16:451–457. [PubMed: 15261679]

Selzer PM, Pingel S, Hsieh I, Ugele B, Chan VJ, Engel JC, et al. Cysteine protease inhibitors as chemotherapy: lessons from a parasite target. Proc Natl Acad Sci. 1999; 96:11015–11022. [PubMed: 10500116]

Sevova ES, Bangs JD. Streamlined architecture and glycosylphosphatidylinositol-dependent trafficking in the early secretory pathway of African trypanosomes. Mol Biol Cell. 2009; 20:4739–4750. [PubMed: 19759175]

Shimamura M, Hager KM, Hajduk SL. The lysosomal targeting and intracellular metabolism of trypanosome lytic factor by *Trypanosoma brucei brucei*. Mol Biochem Parasitol. 2001; 115:227–237. [PubMed: 11420109]

Steverding D, Stierhof YD, Chaudhri M, Ligtenberg M, Schell D, Beck-Sickinger AG, Overath P. ESAG 6 and 7 products of *Trypanosoma brucei* form a transferrin binding protein complex. Eur J Cell Biol. 1994; 64:78–87. [PubMed: 7957316]

Tazeh NN, Bangs JD. Multiple motifs regulate trafficking of the LAMP-like protein p67 in the ancient eukaryote *Trypanosoma brucei*. Traffic. 2007; 8:1007–1017. [PubMed: 17521380]

Tazeh NN, Silverman JS, Schwartz KJ, Sevova ES, Sutterwala SS, Bangs JD. Role of AP-1 in developmentally regulated lysosomal trafficking in *Trypanosoma brucei*. Eukaryot Cell. 2009; 8:1352–1361. [PubMed: 19581441]

Triggs VP, Bangs JD. Glycosylphosphatidy-linositol-dependent protein trafficking in bloodstream stage *Trypanosoma brucei*. Eukaryot Cell. 2003; 2:76–83. [PubMed: 12582124]

Tschudi C, Ullu E. Polygene transcripts are precursors to calmodulin mRNAs in trypanosomes. EMBO J. 1988; 7:455–463. [PubMed: 3366120]

Vanhamme L, Paturiaux-Hanocq F, Poelvoorde P, Nolan DP, Lins L, Van den Abbeele J, et al. Apolipo-protein L-I is the trypanosome lytic factor of human serum. Nature. 2003; 422:83–87. [PubMed: 12621437]

Vanhollebeke B, De Muylder G, Nielsen MJ, Pays A, Tebabi P, Dieu M, et al. A haptoglobin-hemoglobin receptor conveys innate immunity to *Trypanosoma brucei* in humans. Science. 2008; 320:677–681. [PubMed: 18451305]

Vanlandingham PA, Ceresa BP. Rab7 regulates late endocytic trafficking downstream of multivesicular body biogenesis and cargo sequestration. J Biol Chem. 2009; 284:12110–12124. [PubMed: 19265192]

Vickerman K. The fine structure of *Trypanosoma congolense* in its bloodstream phase. J Protozool. 1969; 16:54–69. [PubMed: 4896668]

Wichmann H, Hengst L, Gallwitz D. Endocytosis in yeast: evidence for the involvement of a small GTP-binding protein (Ypt7p). Cell. 1992; 71:1131–1142. [PubMed: 1473149]

Wirtz E, Leal S, Ochatt C, Cross GA. A tightly regulated inducible expression system for conditional gene knock-outs and dominant-negative genetics in *Trypanosoma brucei*. Mol Biochem Parasitol. 1999; 99:89–101. [PubMed: 10215027]

Wollert T, Hurley JH. Molecular mechanism of multivesicular body biogenesis by ESCRT complexes. Nature. 2010; 464:864–869. [PubMed: 20305637]

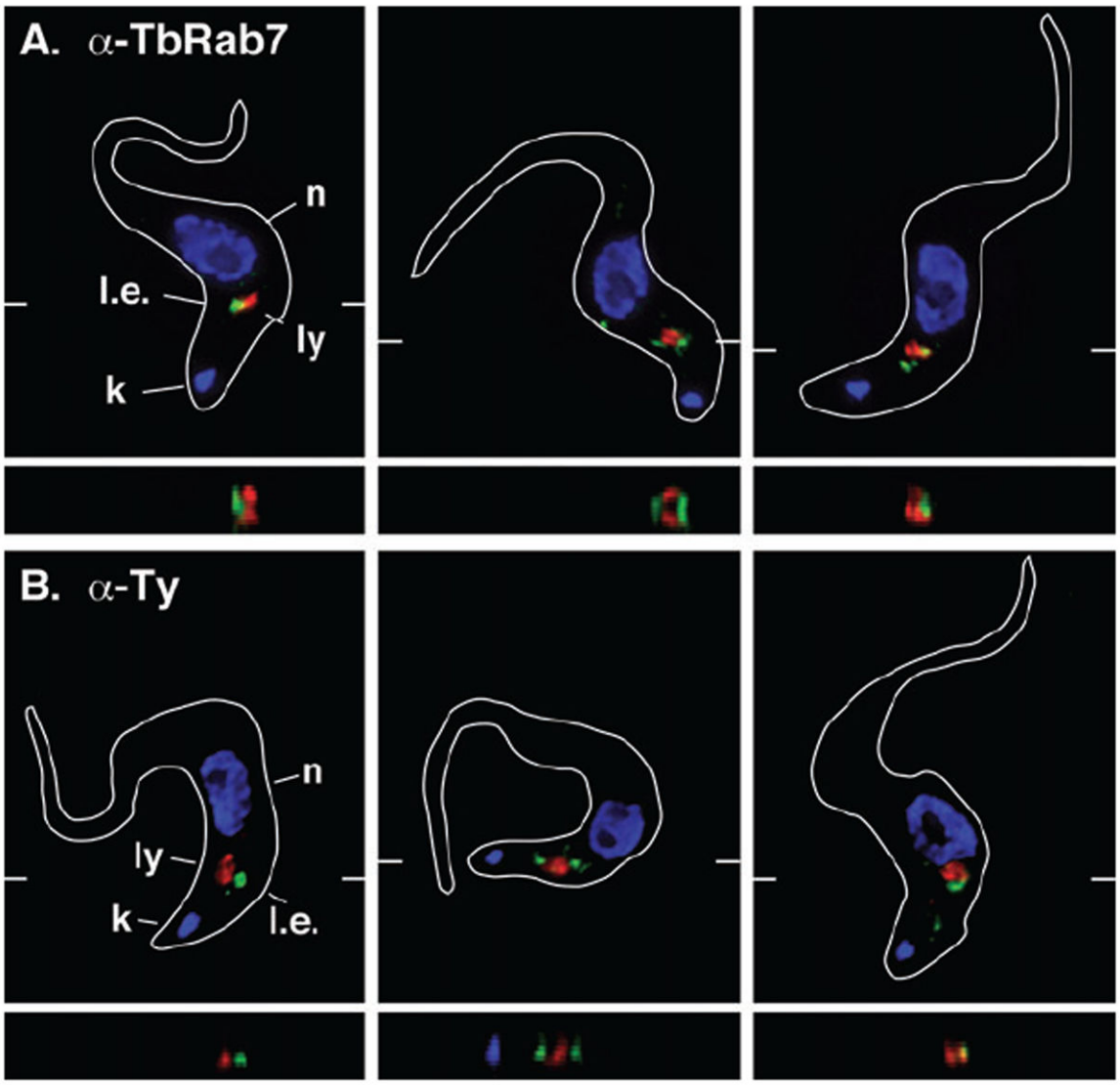

Fig. 1.

Localization of TbRab7 in BSF trypanosomes.

Immunofluorescence microscopy was performed on fixed/permeabilized parental BSF cells (A) or a Ty:TbRab7 *in situ* epitope tagged cell line (B), using anti-TbRab7 or anti-Ty (green) and anti-p67 (red). Three representative images are presented for each cell line. The positions of nuclei (n), kinetoplasts (k), lysosomes (ly), and late endosomes (l.e.) are indicated (left panels only). Merged three-channel summed stack projections (top), and z transects through the lysosome (bottom) are shown. Hatch marks in the xy images signify the plane of the matching z transect. Cell outlines were traced from corresponding differential interference contrast images.

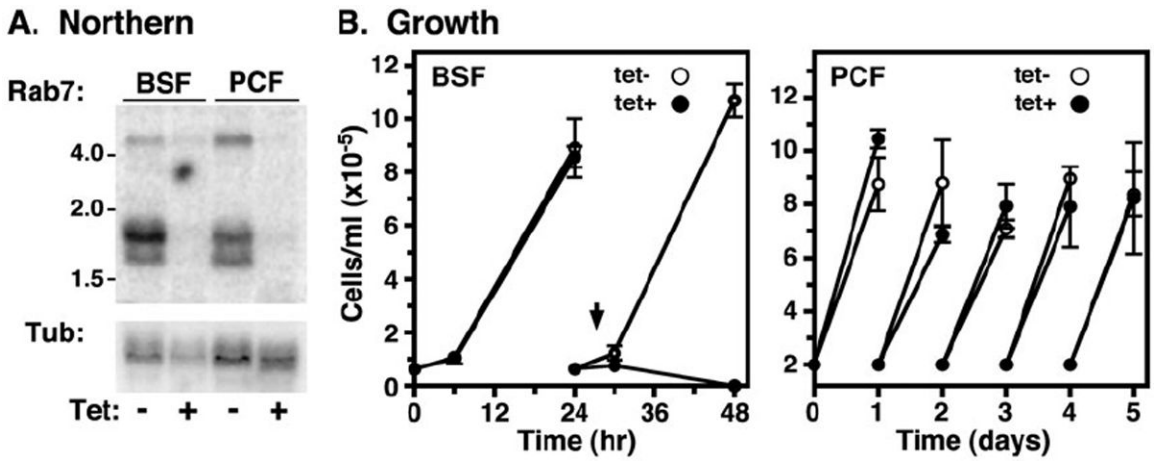

Fig. 2.

TbRab7 RNAi with BSF and PCF trypanosomes. BSF and PCF TbRab7 RNAi cell lines were cultured without or with tetracycline to induce specific knockdown.

A. Northern blot analysis of TbRab7 transcript levels. A representative blot (10 μg total RNA/lane) was probed for TbRab7 transcript (top), stripped, and reprobed for tubulin transcript as a loading control (bottom). Mobilities of size markers are indicated (kb). Analyses were performed after 28 h (BSF) and 72 h (PCF) of induction. Signal levels were quantified by phosphorimaging.

B. Cell density over time was determined by haemocytometer and cells were adjusted to starting density daily. Data are presented as means ± SEM (n = 3). All subsequent RNAi phenotypic analyses reported herein were performed at 28 h in BSF cells (arrowhead).

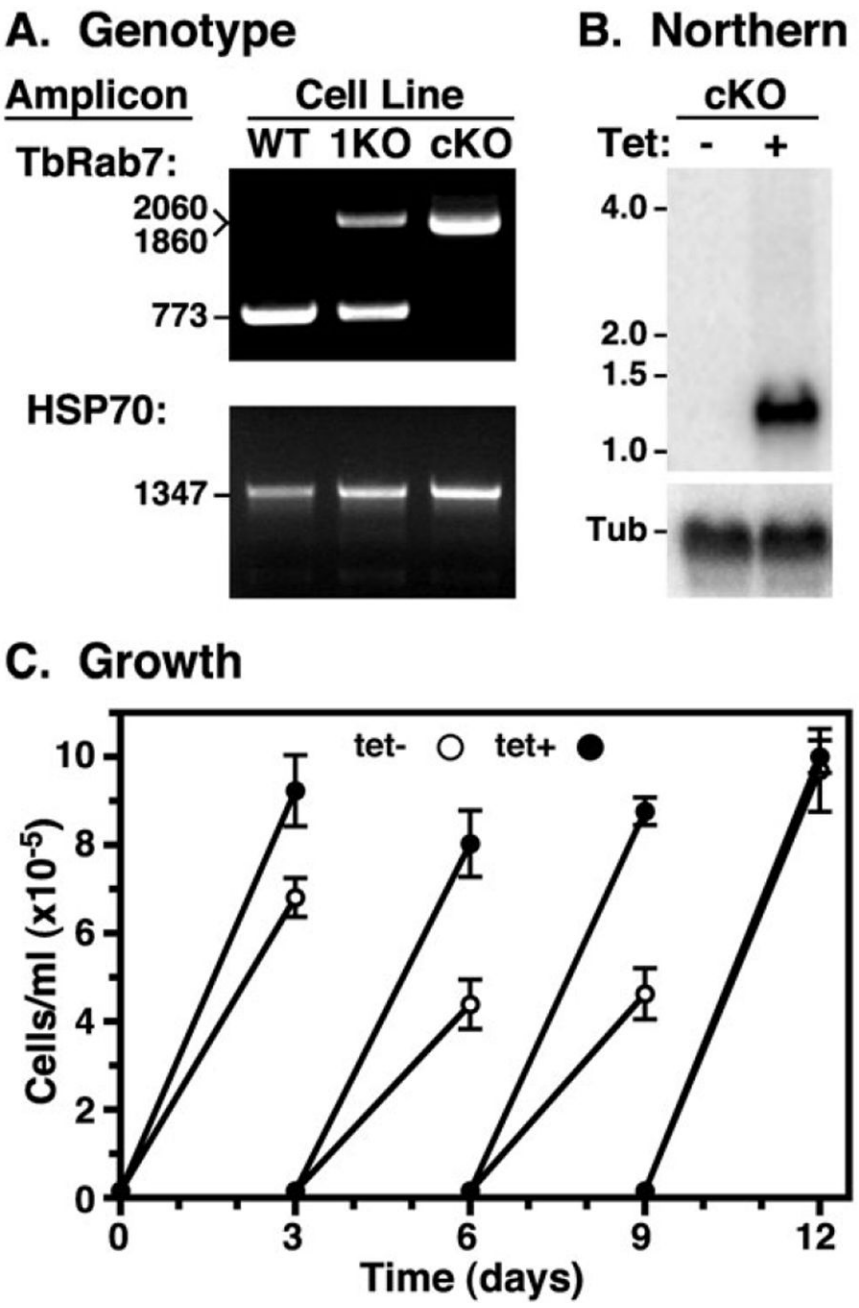

Fig. 3.

Conditional knockout of the TbRab7 locus in PCF trypanosomes.

A. Using flanking primers the TbRab7 locus was PCR amplified from PCF wild type (WT), TbRab7 single knockout (1KO) and TbRab7 conditional double knockout (cKO) genomic DNA. The HSP70 orf was also amplified as a positive control for amplification and loading. PCR products were fractionated on 0.8% agarose gels. Sizes of PCR products are indicated (nts). Note that PCR products of the first round (2060 nts) and second round (1860 nts) allelic replacement constructs are close in size.

B. Total RNA (10 μg/lane) from the PCF cKO cell line grown in the absence (−) and presence (+) of tetracycline for 6 days was probed for TbRab7 mRNA as in Fig. 2. The blot was stripped and reprobed for tubulin as a loading control.

C. Growth curves of the PCF cKO cell line in the absence and presence of tetracycline. Cultures were adjusted to starting cell density every 3 days. Data are presented as means ± SEM (n = 3).

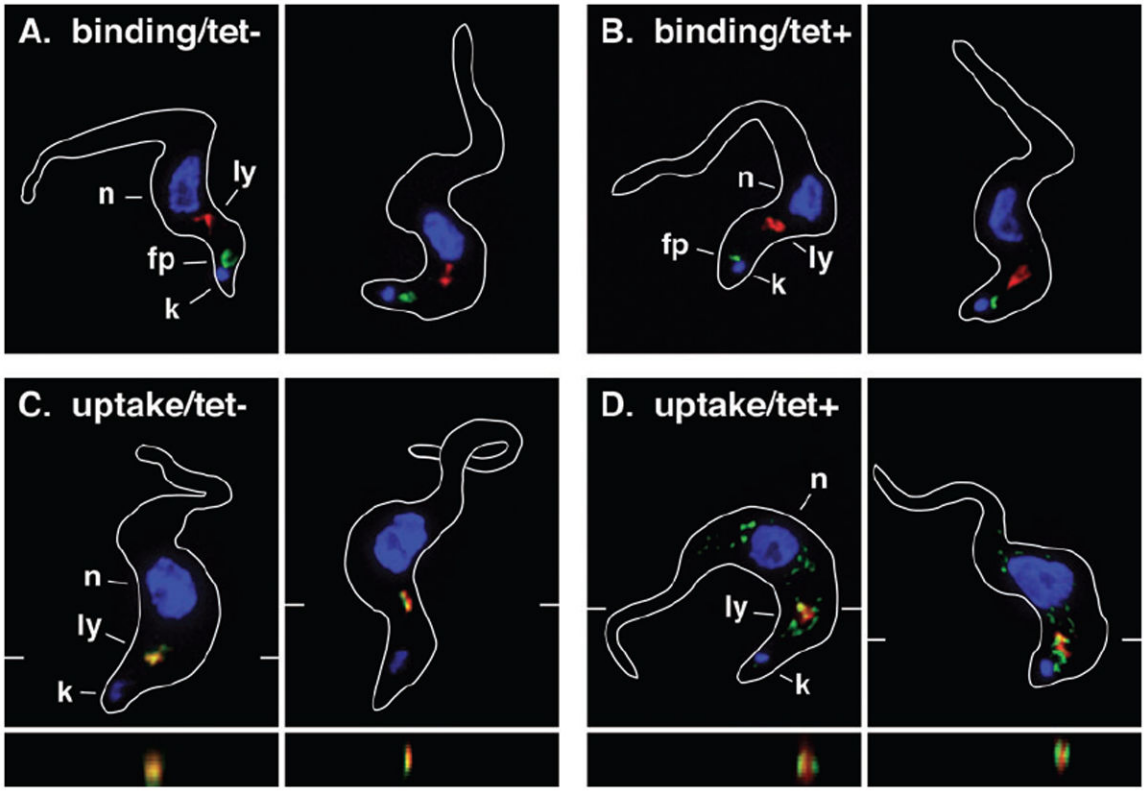

Fig. 4.

Effect of TbRab7 silencing on endocytosis (I). Control (A & C, tet−) and TbRab7 silenced (B & D, tet+) BSF cells were assayed for tomato lectin:biotin conjugate (TL:Bio) binding (A & B) and uptake (C & D). For binding cells were incubated with TL:Bio (5°C, 30 min) to label the flagellar pocket, and then processed for immunofluorescence. Alternatively, cells were incubated with TL:Bio (37°C, 30 min) to allow continuous endocytosis to occur and then chased (20 min) before processing for immunofluorescence. (All Panels) Fixed/permeabilized cells were stained with anti-p67 (red) and TL:Bio was detected with SA:488 (green). The positions of nuclei (n), kinetoplasts (k), lysosomes (ly), and flagellar pockets (fp) are indicated (left panels only). Representative three-channel summed stack projections are presented. Cell outlines were traced from matched differential interference contrast images (not shown). Z-plane transects through the lysosomes (bottom, C & D only) are indicated by marginal hatch marks in the corresponding xy images.

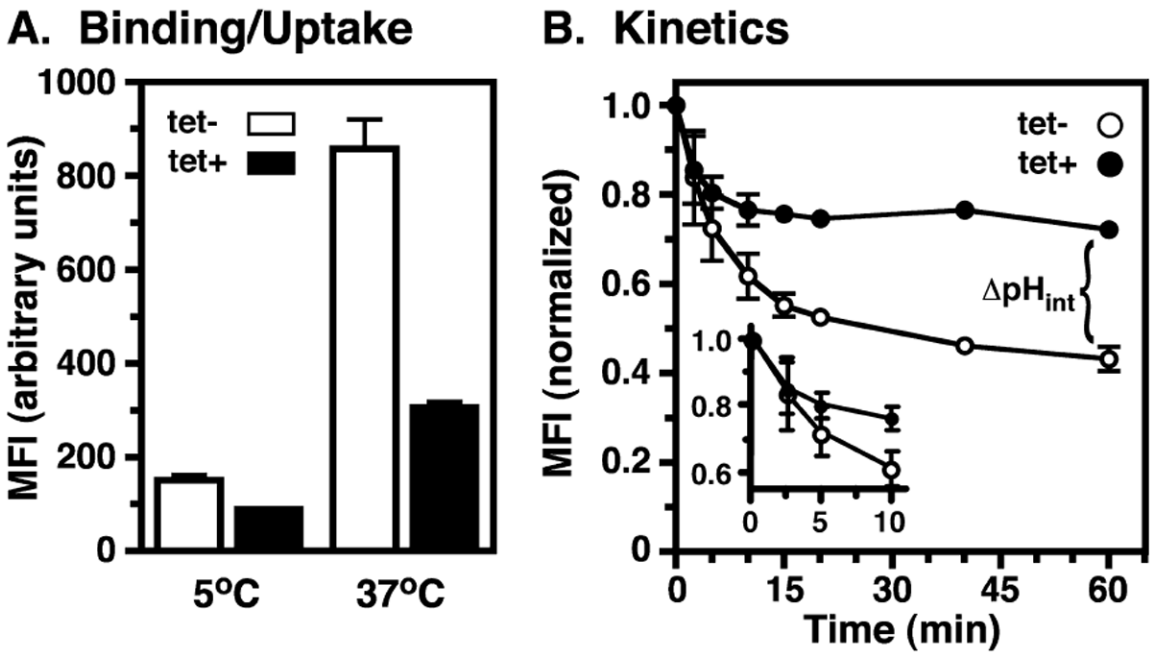

Fig. 5.

Effect of TbRab7 silencing on endocytosis (II). Control (tet−) and TbRab7 silenced (tet+) BSF cells were incubated with fluorescent tomato lectin conjugates and flow cytometry was performed.

A. Cells were incubated with TL:A488 to allow either flagellar pocket binding or uptake as in Fig. 4, and cell associated fluorescence was assessed by flow cytometry. Mean fluorescent intensities (MFI) are presented (means ± SEM, $n = 6$). Unpaired t-tests indicated significant differences ($P < 0.0005$) between control vs. silenced cells for both binding and uptake.

B. To determine kinetics of endocytosis, cells were incubated with pH-sensitive TL:FITC (5°C, 30 min), washed, shifted to 37°C in fresh media, and fluorescence measured over time by flow cytometry. Data are normalized to initial bound ligand and are presented as MFI (means ± SEM, $n = 3$). Insert graph is an expansion of the early time points of endocytosis.

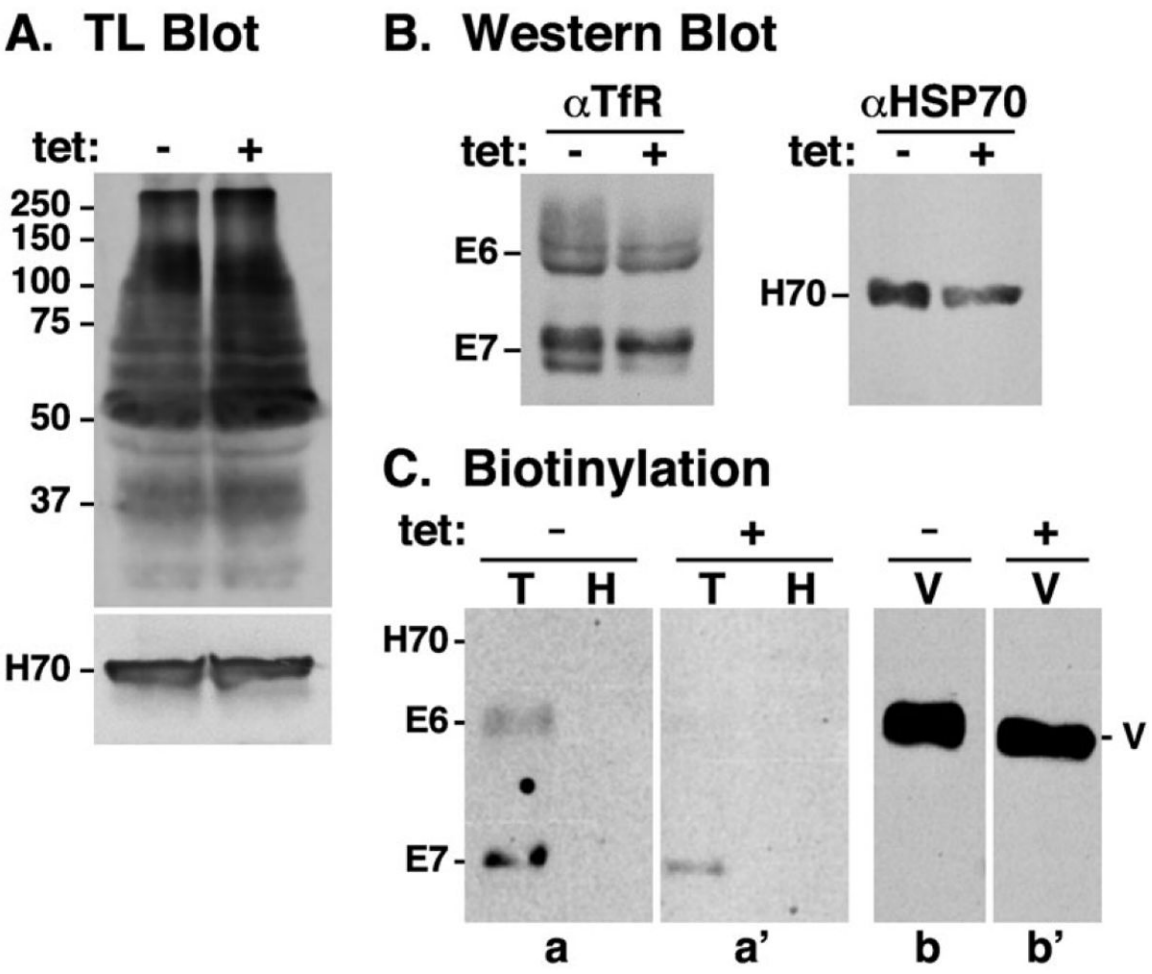

Fig. 6.

Downregulation of cell surface transferrin receptor. pNAL modification and TfR distribution was investigated in control (tet−) and TbRab7 silenced (tet+) cells.

A. Total extracts of control and silenced TbRab7 RNAi cells were fractionated by SDS-PAGE (10^7 cells/lane) and transferred to membranes. Membranes were blotted first with anti-HSP70 as a loading control, stripped and then blotted with TL. Molecular weight markers are indicated in kDa.

B. Total cell extracts (10^7 cells/lane) were immunoblotted with anti-TfR antibody. Blot was stripped and reprobed with anti-HSP70 as a loading control.

C. Intact control and silenced TbRab7 RNAi cells were surface biotinylated as described in *Experimental procedures*. Polypeptides were immunoprecipitated with anti-TfR (T), anti-HSP70 (H, control negative), and anti-VSG221 (V, control positive). After fractionation by SDS-PAGE (TfR & HSP70, 10^7 cell equivalents/lane; VSG221, 5×10^4 cell equivalents/lane), and membrane transfer, blotting was performed with SA:HRP. All lanes are from the same gel, blot and film, but have been reordered for the purpose of presentation. Sections a & a', and b & b', were digitally contrasted identically before rearrangement. (A–C) Mobilities of the ESAG6 (E6) and ESAG7 (E7) subunits of TfR, HSP70 (H70) and VSG (V) are indicated.

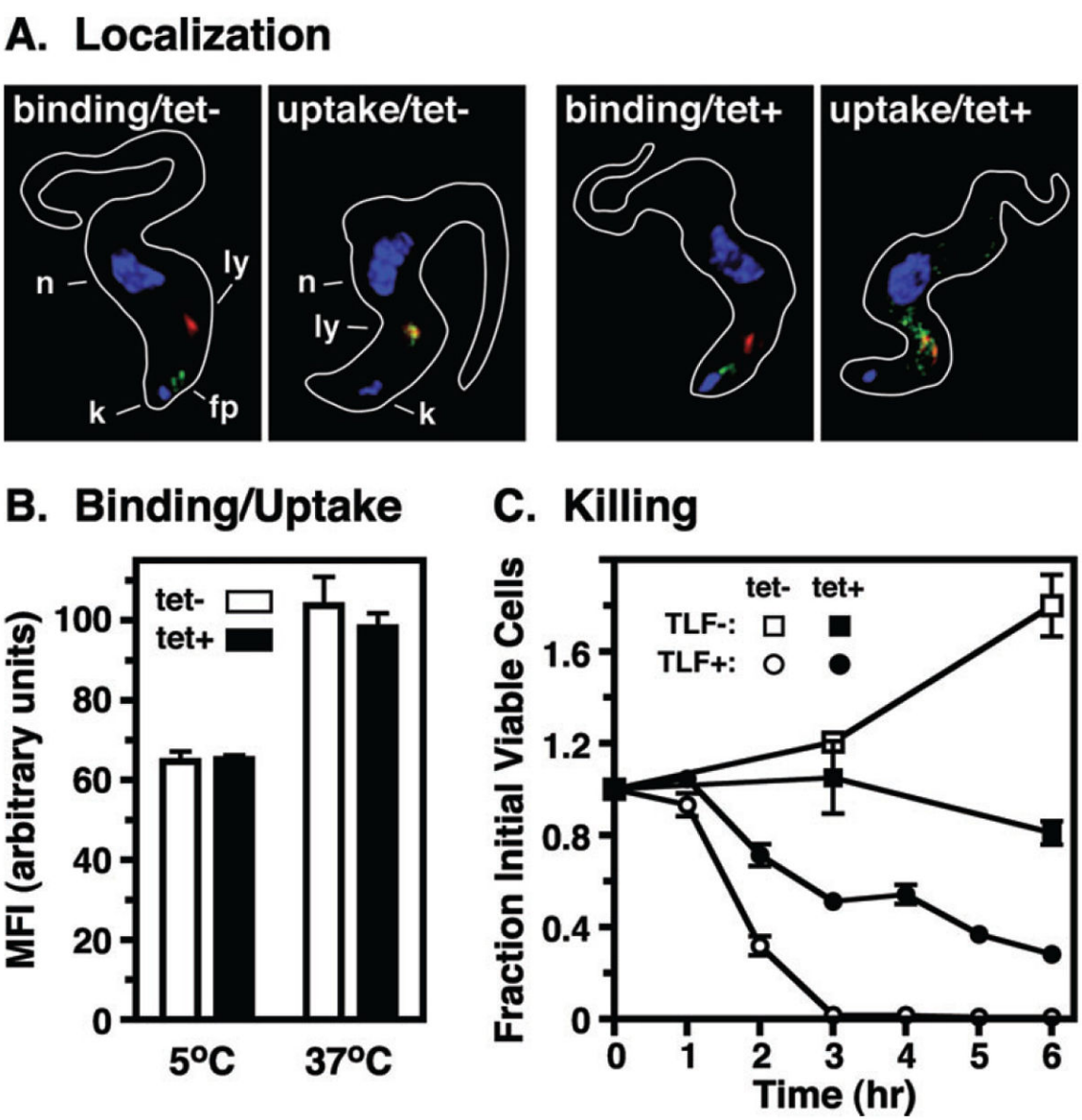

Fig. 7.

Effect of TbRab7 silencing on TLF killing. Control (tet−) and TbRab7 silenced (tet+) BSF cells were incubated with purified TLF. Cells were incubated with TLF:A488 for flagellar pocket binding and uptake as in Fig. 4.

A. For microscopy cells were fixed/permeabilized and stained with anti-p67 (red) and TLF:A488 was detected directly (green). The positions of nuclei (n), kinetoplasts (k), lysosomes (ly), and flagellar pockets (fp) are indicated (control only). B. Cell associated fluorescence in fixed cells was quantitatively assessed by flow cytometry. Mean fluorescent intensities (MFI) are presented (means ± SEM, $n = 6$). Unpaired *t*-tests indicated no significant differences ($P > 0.5$) between control vs. silenced cells for both binding and uptake. C. TLF killing. Cells were incubated at 37°C with or without unconjugated TLF. Cell death was scored by phase microscopy and is presented over time as fraction of initial viable cells (means ± SEM, $n = 3$). Rate of killing was determined as the slope (m)

following regression analysis over the linear phase (control, 1–3 h, m = 45.7%/h, r^2 = 0.9440; silenced, 1–6 h, m = 13.8%/h, r^2 = 0.8562).

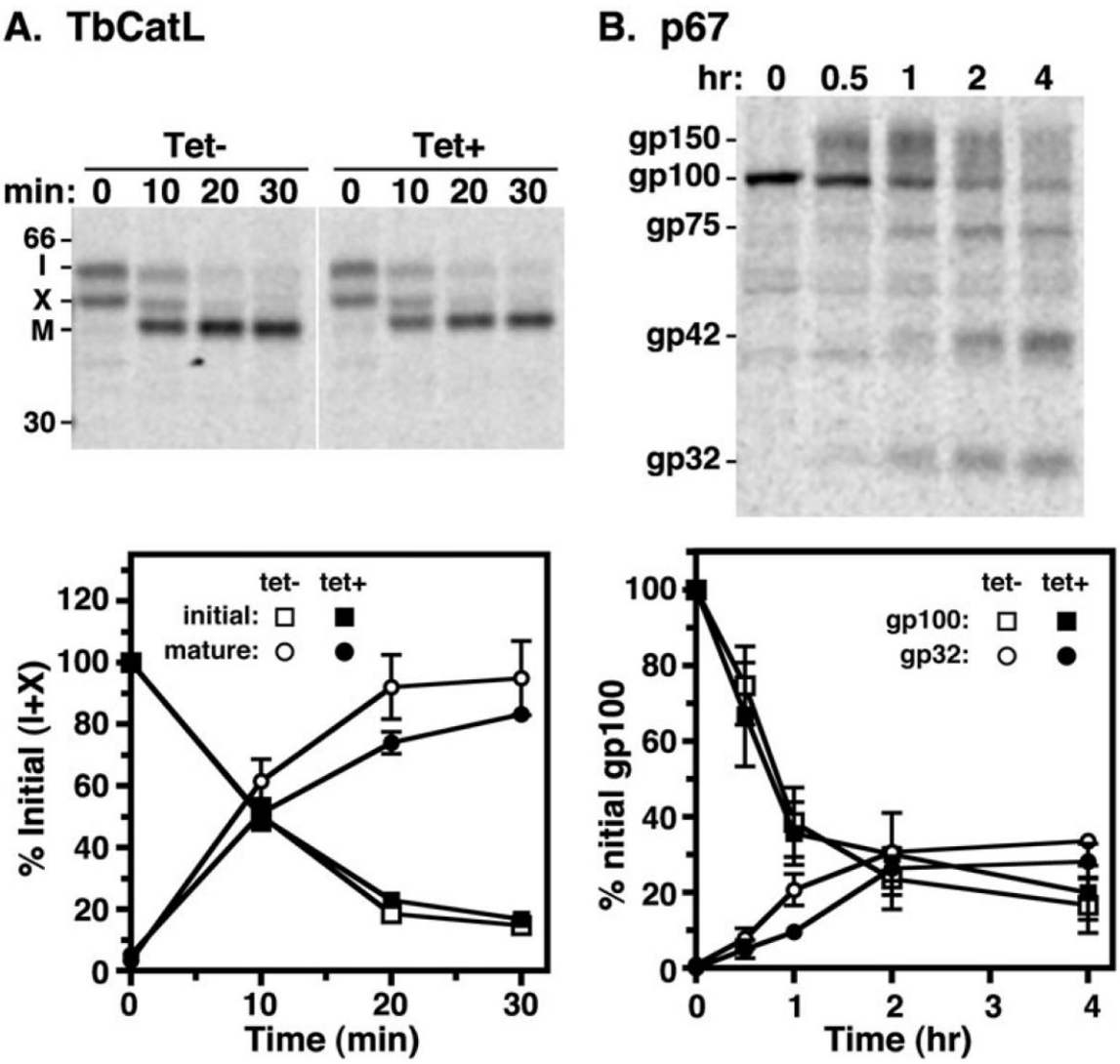

Fig. 8.

Biosynthetic trafficking of endogenous lysosomal cargo. Pulse-chase analysis of TbCatL (A) and p67 (B) trafficking was performed on control (tet−) and TbRab7 silenced (tet+) BSF cells. (A, top) Radiolabelled TbCatL was specifically immunoprecipitated from cell lysates at the indicated chase times, fractionated by SDS-PAGE (10^7 cell equivalents/lane), and visualized by phosphorimaging. A representative image is presented with mobilities of immature proprotein (I), uncharacterized precursor form (X), and mature lysosomal form (M) indicated. All lanes are from the same gel/phosphoimage with identical contrasting. Vertical stripe indicates digitally excised irrelevant lanes. (A, bottom) Quantification of TbCatL processing (means ± SEM, $n = 3$). Precursor (I + X) and mature forms (M) are presented as a percentage of initial species (I + X). (B, top) Representative phosphorimage of immunoprecipitated p67 (10^7 cell equivalents/lane) from control cells only. Mobilities of initial ER gp100, Golgi-modified gp150, and quasi-stable lysosomal gp75, gp42, and gp32 glycoforms are indicated. (B, bottom) Quantification p67 processing (means ± SEM, $n = 3$). Data shown are gp100 and gp32 glycoforms presented as a percentage of initial gp100.

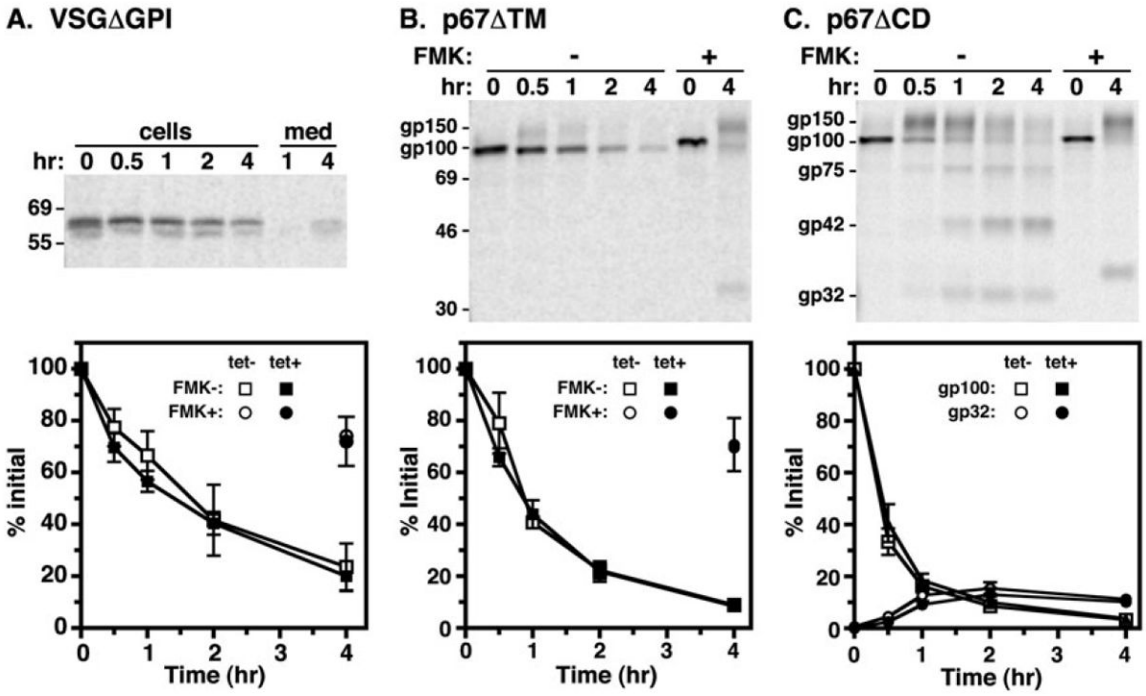

Fig. 9.

Biosynthetic trafficking of default reporters. Pulse-chase analysis was performed (as in Fig. 8) on control (tet−) and TbRab7 silenced (tet+) BSF cells constitutively expressing (A) VSG117ΔGPI (B) p67ΔTM and (C) p67ΔCD default reporters. In each case radiolabelled reporter polypeptides were specifically immunoprecipitated from equivalent cell lysate and media fractions (A) or cell extracts only (B & C). p67ΔTM and p67ΔCD have C-terminal 3xHA tags and were immunoprecipitated with anti-HA to avoid background from endogenous p67. (Top) Representative phosphorimages of immunoprecipitated reporter polypeptides (10^7 cell equivalents/lane) from control cells are presented. Mobilities of p67 glycoforms and selected molecular weight markers (kDa) are indicated. (Bottom) Quantification of cell-associated reporter polypeptides from pulse-chase assays of control and silenced cells (means ± SEM, $n = 3$). Recoveries are quantified as percentage of initial reporter. Also presented is recovery at 4 h in cells assayed in the presence of the lysosomal cysteine protease inhibitor FMK024 (20 μM).